

The Interaction Between Pilot Based Linear Equalizer and Device Nonlinearity in Optical Coherent Communication

Xiaofei Su^{(1) *}, Ke Zhang⁽¹⁾, Tong Ye⁽¹⁾, Zhenning Tao⁽¹⁾, Hisao Nakashima⁽²⁾, Takeshi Hoshida⁽²⁾

⁽¹⁾ Fujitsu R&D Center, No. 8 Jian Guo Men Wai Ave., Beijing, China, suxiaofei@fujitsu.com

⁽²⁾ Fujitsu Ltd., 1-1 Shin-ogura, Saiwai-Ku, Kawasaki 212-8510, Japan

Abstract *The interaction between QPSK pilot based linear equalizer and device nonlinearity and the corresponding penalty are demonstrated experimentally. By setting proper amplitude probabilistic distribution, new pilot design mitigates it and improves Q more than 1dB.*

Introduction

Due to the increasing demands of spectrum efficiency and transmission capacity, high baud rate and high-order modulation formats, such as 100 GBaud 64-QAM^[1], are considered in optical communication. In such high-speed systems, the devices, including driver, modulator and so on, require high bandwidth, which always have non-negligible nonlinearity^[2]. This nonlinearity brought negative effects to the system performance.

At present, the adaptive equalizer (AEQ) for high-order modulation format (e.g., 64-QAM) is always based on QPSK (quadrature phase shift keying) pilot^{[3]-[4]}. As we know, for linear transmissions, the AEQ coefficients estimated by QPSK pilot can equalize the 64QAM payload well. However, for the system with nonlinearity, the situation will become more complicated. In nonlinear case, are the AEQ coefficients estimated by QPSK pilot still the optimal ones for high order modulated payload? To improve the performance of high order modulated system with nonlinearity, this question should be clearly discussed.

In this paper, we analyse the interaction between pilot sequence (PS) based AEQ and device nonlinearity in detail. Experiments show that, the adaptive equalizer obtained by conventional PS is indeed no longer the optimal one for payload in nonlinear case. To overcome this drawback, the new PS designs with proper amplitude probability distribution function (PDF) are proposed. Compared with the outer ring PS design which is used in OIF-400G ZR^[5], more than 1 dB Q improvement is achieved.

Interactions between nonlinearity and AEQ

Fig. 1 shows the experiment setup and Rx DSP flow. The transmitted signal is 44 GBaud DP-64QAM signal with root-raised-cosine pulse shaping (roll-off factor of 0.15), in which 256-symbol TS (training sequence) is added in

each frame and 1-symbol PS is periodically inserted with the ratio of 1/32. Following 88 GSa/s DAC, coherent driver modulator (CDM) is used to modulate the amplified electrical signal to optical field. The RF driver which is the main nonlinear device, works at the gain control model and the gain is about 17.6 dB.

The receiver includes a local oscillator, dual-polarization 90-degree hybrid, balanced photodiodes, and DSO (digital storage oscilloscope) operating at 80 GSa/s with 33 GHz bandwidth. The nonlinear effect in such receiver is negligible. The stored signals are then processed in off-line DSP which carries out re-sampling, Rx I/Q imbalance compensation, training sequence based frame synchronization, PS based 57-tap CMA equalization, frequency offset compensation, PS based carrier phase recovery, and Tx imbalance compensation employing PS based 4*4 MMSE equalization with tap number of 5. For the PS with multi-level amplitude, such as 64QAM PS, the multi-amplitude CMA or the classic CMA^[6] is used. The initial tap coefficients of CMA come from the linear equalizer estimated by periodic CAZAC (constant envelope zero autocorrelation sequence) in training sequence.

The nonlinear characteristic strongly depends on input signal power^[7]. To illustrate the nonlinear conditions intuitively, we feed digital two-tone signal with different power into the modulator and measure the power ratio between the 3rd order intermodulation (IM3) and the fundamental tone (FUND) at output. The ratios are shown in Fig. 2, whose variation is about 14 dB. The maximum FUND/IMD3 reaches up to 28.7 dB, which represents the corresponding condition is approximately linear. The minimum ratio is 15 dB, which implies significant nonlinear condition.

For comparison, the AEQ scheme which use periodically inserted 64-QAM pilot (named as 64QAM PS) is operated to obtain the reference performance. The

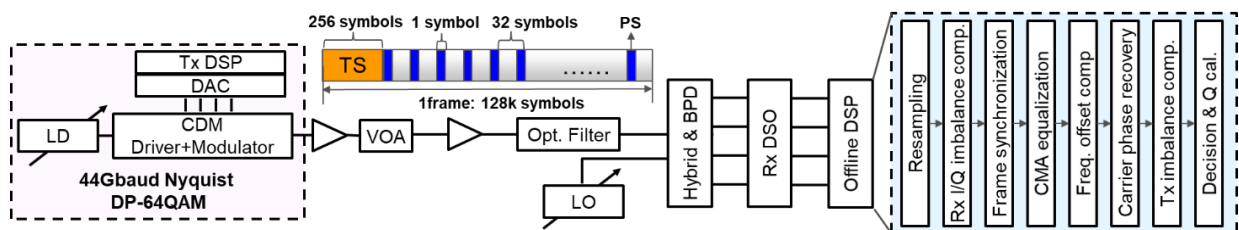


Fig. 1: Experiment setup of optical back-to-back system. LD: Laser diode, DAC: Digital-to-analog converter, CDM: Coherent driver modulator, VOA: Variable optical attenuator, LO: Local oscillator, BPD: Balance photodiode, TS: Training sequence.

conventional PS scheme, including widely used QPSK PS with same mean-power as payload (named same-power PS) and outer ring PS suggested by OIF standard, are also investigated. The results are shown in Fig. 3. In approximate linear condition (DAC input RMS = 21.7, IM3 power ratio = 28.7 dB), 3 PS schemes catch similar Q performance, and all the Q differences are less than 0.2 dB. But along with nonlinearity increasing, the performances of 2 conventional single-amplitude PS have significant Q penalty. Compared with 64QAM PS, the maximum Q penalty is up to 0.65 dB and 1.86 dB for same-power PS and outer ring PS, respectively. The interaction between linear equalizer and nonlinear effect exists clearly.

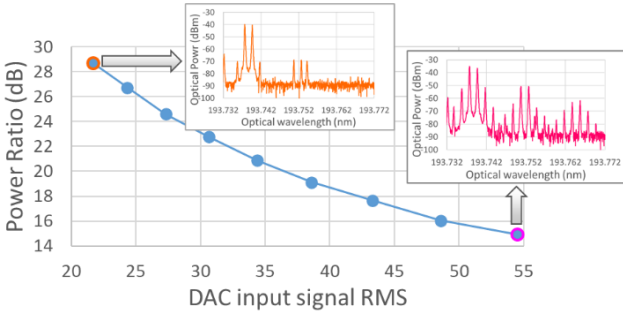


Fig. 2: Power ratio between 3rd order intermodulation (IM3) and fundamental tone (FUND) vs. DAC input signal RMS. DAC full swing: -127~127

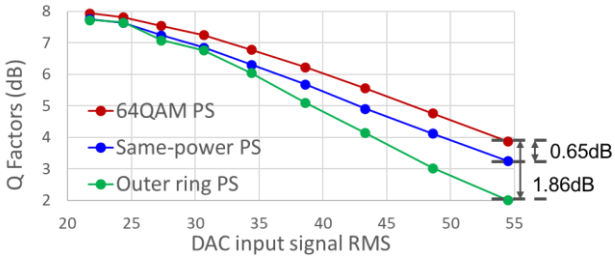


Fig. 3: Q factors vs. DAC input signal RMS for single-amplitude PSs and 64QAM PS

Design of new pilots

Different pilots assisted AEQs perform different Q values, that is mainly caused by the fact that the PDF of different pilots are quite different. According to the theory of BLA (best linear approximation), the optimal linear filter is affected by the PDF of input signal in nonlinear system^{[8]-[9]}. For instance, the best linear filter for Gaussian-distributed signal or NRZ signal are not same^[10]. Thus, to guarantee the optimal AEQ coefficients for payload, the pilots should have similar PDF, at least similar PDF of amplitude, with payload.

Based on this, we propose the first PS design, which has the same amplitude PDF with payload (named as same-PDF PS). Take 64-QAM payload as an example, the amplitude PDFs and constellation diagrams of payload and PS are shown in Fig. 4. The proposed pilot sequency have 9 amplitude level in total. The phases of each level symbols are same with those of QPSK format because this PS is also used for carrier phase recovery.

However, same-PDF PS does not locate on the payload constellation, and the implementation may be difficult. Thus, we propose another pilot design, whose

low order origin moments are as same as payload (named as same-moment PS). Compared with same-PDF pilot, same-moment PS also contains multi-amplitude QPSKs, but all the points are located at payload constellation points. The PS original moments are adjusted by the probability of PS with different amplitude level. One example is shown in Fig. 5, for 64-QAM payload, the amplitude level of same-moment PS is decreased to 4. The probability of different amplitude level of same-moment PS, the low order origin moments of 64-QAM and designed same-moment PS are shown in Fig. 5.

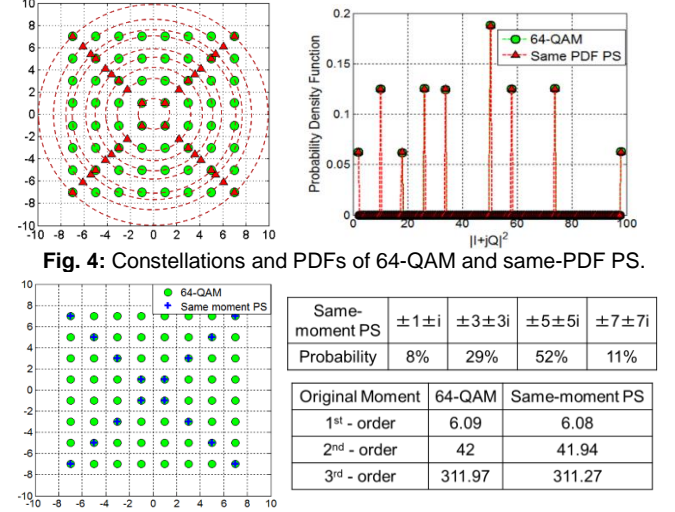


Fig. 4: Constellations and PDFs of 64-QAM and same-PDF PS.

Fig. 5: Constellation and origin moment for 64-QAM and same-moment PS, and amplitude probability for same-moment PS.

Performance analysis

Fig. 6 shows the Q factors vs. DAC input signal RMS for all the PSs, including 2 multi-amplitude PSs, 2 single-amplitude PSs, and reference 64QAM PS. The proposed 2 multi-amplitude PSs have similar Q performance, which are all close to the reference Q using 64QAM PS.

In non-negligible nonlinear cases (DAC input RMS = 43.29, IM3 power ratio = 17.66 dB), where the reference Q (5.69 dB) reach 20% FEC limitation^[11], the proposed PS schemes has more than 0.5 dB and 1.27 dB Q improvement compared with same-power PS scheme and outer ring PS scheme, respectively.

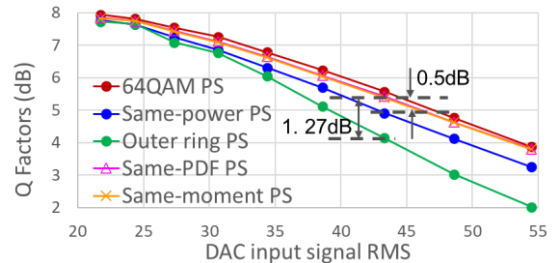


Fig. 6: Q factors vs. DAC input signal RMS for 5 kinds of PS.

To further investigate the mechanism of AEQ-nonlinear interaction, we analyse the CMA tap coefficients and Euclidean distance error for different pilots, in both approximate linear and significant nonlinear condition.

1. Discussion in linear condition

In linear condition (DAC input RMS = 21.7, IM3 power ratio = 28.7 dB), the tap coefficients of adaptive

equalizers that optimized by different PSs are similar. As Fig. 7 shows, the AEQ frequency spectra for 5 PSs are close to each other. It can be concluded that, for both conventional single-amplitude PSs and proposed PSs, the adaptive equalizers estimated by pilot are all optimal for payload in linear condition.

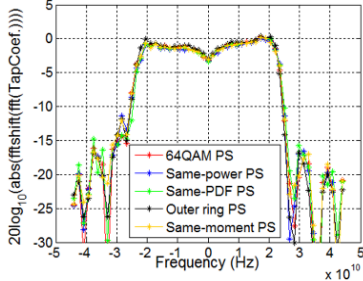


Fig. 7: Frequency spectrum response of AEQ applying different PS in linear condition.

2. Discussion for conventional PS in nonlinear condition

Here we choose the DAC input RMS = 43.29 (IM3 power ratio = 17.66 dB) case as nonlinear condition. To analyse the AEQ performance of different PSs, we calculate the statistical Euclidean distance error (defined as $E[(y - s)^2]$, y is the equalized output symbol, s is the input symbol) for both pilot symbols and payload symbols. Tab. 1 gives the Euclidean distance error and Q results by using 64QAM PS, same-power PS and outer ring PS assisted AEQ, respectively. When AEQ optimized by reference 64QAM PS, the Euclidean distance error statistical of pilot is similar with that of payload. This proves that the AEQ optimized by 64QAM PS is the optimal equalizer for payload. But for QPSK PS with same-power and PS located on outer ring, the Euclidean distance error statistical on pilot is smaller than that of 64QAM PS, and this indicates AEQ works well. However, the error of payload for same-power PS and outer ring PS is larger than that for 64QAM PS and the Q value is lower. It reveals that the single-amplitude pilot assisted AEQ just minimize the error of pilot, while this optimization is not the optimal equalizer for payload. This is the mechanism of AEQ-nonlinear interaction.

Tab. 1: Euclidean distance error for 64QAM PS and 2 single-amplitude PSs.

Pilot type	Pilot error	Payload error	Q (dB)
64QAM PS	0.592	0.681	5.69
Same-power PS	0.403	0.806	5.06
Outer ring PS	0.576	0.927	4.29

Tab. 2: Euclidean distance error for 64QAM PS and 2 proposed multi-amplitude PSs.

Pilot type	Pilot error	Payload error	Q (dB)
64QAM PS	0.592	0.681	5.69
Same-PDF PS	0.516	0.708	5.56
Same-moment PS	0.512	0.708	5.56

The AEQ tap coefficients also support above mechanism. Fig. 8 compares the frequency spectrum response of AEQ tap coefficients estimated by reference 64QAM PS and 2 kinds of single amplitude PS. For each iteration, the initial tap coefficients of AEQ are same, and

the convergence results are shown in Fig. 8 (a). Tap coefficients of single-amplitude PSs assisted AEQ are deviated from the reference tap coefficients of AEQ aligned on 64QAM PS (red curve), which causes Q difference. This deviation clearly indicates the interaction between single amplitude PS based AEQ and device nonlinearity.

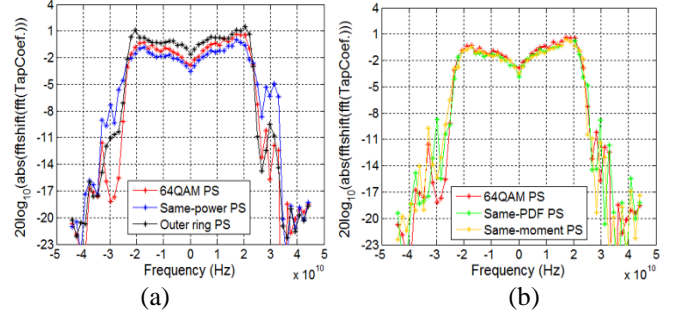


Fig. 8: Frequency spectrum response of AEQ applying 64QAM PS and 2 single-amplitude PSs (a), and applying 64QAM PS and 2 multi-amplitude PSs (b) in nonlinear condition.

3. Discussion for proposed PS in nonlinear condition

We also analyse the Euclidean distance error and frequency spectrum response of proposed multi-amplitude PSs. In Tab. 2, the Q values of 2 proposed PSs are almost same with reference Q (5.69 dB). For each PS scheme, the statistical Euclidean distance error for payload is similar. In addition, the frequency magnitude difference of AEQ coefficients for proposed and reference PS schemes is within 0.6 dB over the signal bandwidth, as shown in Fig. 8 (b). It is apparent that the new pilots can estimate the optimal equalizer for payload in adaptive equalization.

In view of practical applications, we recommend the same-moment PS because the PS locates on the payload constellation.

Conclusion

In this paper, we intensively analyse the interaction between pilot based adaptive equalizer and device nonlinearity. Experiments show that in nonlinear condition, the adaptive equalizer optimized for conventional single-amplitude pilot sequence is no longer the optimal equalizer for payload. The maximum Q penalty is up to 0.65 dB and 1.86 dB for conventional PSs with same mean-power as payload and same power as outer ring, respectively.

To immune the performance penalty, we proposed new pilot designs by proper amplitude PDF. Unlike conventional pilots, the proposed ones can achieve the optimal equalizer for payload. By applying new pilots, the Q penalty of conventional PS is removed. Considering the practical implementation, PS with same low-order origin moment is proposed.

References

- [1] Schuh K, et al. 'Single Carrier 1.2 Tbit/s Transmission over 300km with PM-64 QAM at 100 GBaud', OFC, Los Angeles, USA, 2017, Th5B.5.
- [2] Verbist, et al. '112 Gbit/s Single-Polarization Silicon Coherent Receiver with Hybrid-Integrated BiCMOS Linear TIA', ECOC, Valencia, Spain, Sept. 2015, P.4.15.

- [3] Yankov M P, et al, 'Experimental analysis of pilot-based equalization for probabilistically shaped WDM systems with 256QAM/1024QAM', OFC, Los Angeles, USA,2017, W2A.48.
- [4] Y. Fan, et al. 'Calibration and monitoring of coherent optical transceiver imperfections', Next-Generation Optical Communication. San Francisco, USA, 2020, 11309-23.
- [5] <http://openroadm.org/download.html>, OpenROADM_MSA3.01 W-Port Digital Specification.docx, pp47-48.
- [6] X. Zhou and J. Yu, 'Multi-Level, Multi-Dimensional Coding for High-Speed and High-Spectral-Efficiency Optical Transmission', JLT, 2009, Aug.15, vol. 27, no. 16, pp. 3641-3653.
- [7] H. Chen, et al. 'High-accuracy Gain-isolated Volterra Nonlinear Behavior Model for Wideband Driver in Optical Coherent Transmitter', OFC, Anaheim, USA, 2016, Th2A.29.
- [8] Adam C, et al. 'Distortion Contribution Analysis With the Best Linear Approximation', Circuits and Systems I: Regular Papers, IEEE Transactions on, 2018, 65(12):4133-4146.
- [9] Rolain Y, et al. 'A measurement-based error-vector-magnitude model to assess non linearity at the system level', 2017 IEEE/MTT-S International Microwave Symposium - IMS 2017. IEEE, 2017.
- [10] Wong H K, et al. 'Analysis of Best Linear Approximation of a Wiener-Hammerstein System for Arbitrary Amplitude Distributions', IEEE Transactions on Instrumentation & Measurement, 2012, 61(3):645-654.
- [11] K. Sugihara et al., 'A Spatially-coupled Type LDPC Code with an NCG of 12 dB for Optical Transmission beyond 100 Gb/s', OFC, Anaheim, USA, 2013, OM2B.4.